HHS Public Access

Author manuscript

Cancer Res. Author manuscript; available in PMC 2019 January 01.

Published in final edited form as:

Cancer Res. 2018 January 01; 78(1): 230–245. doi:10.1158/0008-5472.CAN-17-1961.

Evidence For Kaposi's Sarcoma Originating From Mesenchymal Stem Cell Through KSHV-induced Mesenchymal-to-Endothelial Transition

Yuqing Li[a,#], **Canrong Zhong**[a,#], **Dawei Liu**[b], **Wenjing Yu**[d], **Weikang Chen**[a], **Yan Wang**[a,c], **Songtao Shi**[d], and **Yan Yuan**[a,e,*]

[a]Institute of Human Virology and Ministry of Education Key Laboratory of Tropical Disease Control, Zhongshan School of Medicine, Sun Yat-sen University

[b]Department of Pathology, The First Affiliated Hospital, Sun Yat-sen University

[c]Guanghua School of Stomatology, Guangdong Provincial Key Laboratory of Stomatology, Sun Yat-sen University, Guangzhou, Guangdong 510080, China

[d]Department of Anatomy and Cell Biology

[e]Department of Microbiology, University of Pennsylvania School of Dental Medicine, Philadelphia, PA 19104, USA

Abstract

The major transmission route for Kaposi's sarcoma-associated herpesvirus (KSHV) infection is the oral cavity through saliva. Kaposi's sarcoma (KS) frequently occurs in the oral cavity in HIV-positive individuals and is often the first presenting sign of AIDS. However, the oral target cells for KSHV infection and the cellular origin of KS remain unknown. Here we present clinical and experimental evidences that KS spindle cells may originate from virally modified oral mesenchymal stem cells (MSC). AIDS-KS spindle cells expressed neuroectodermal stem cell marker (Nestin) and oral MSC marker CD29, suggesting an oral/craniofacial MSC lineage of AIDS-associated KS. Furthermore, oral MSC were highly susceptible to KSHV infection, and infection promoted multi-lineage differentiation and mesenchymal-to-endothelial transition (MEndT). KSHV infection of oral MSCs resulted in expression of a large number of cytokines, a characteristic of KS, and upregulation of KS signature and MEndT-associated genes. These results suggest that KS may originate from pluripotent MSC and KSHV infection transforms MSC to KS-like cells through MEndT.

Introduction

Kaposi's sarcoma (KS) is the most common malignancy associated with HIV-infection. About 20% of AIDS patients develop KS with most of them (60%) manifesting with oral

[*]**Corresponding authors.** Mailing Address: Department of Microbiology, University of Pennsylvania School of Dental Medicine, Philadelphia, PA 19104, Phone: (215) 573-7556; Fax: (215) 898-8385, yuan2@pobox.upenn.edu.
[#]Equal contribution.

Conflict of Interest: The authors declare no potential conflicts of interest.

lesions(1). Oral KS is often the first presenting sign of AIDS and the most common intraoral KS sites are palate and gingiva (1). Furthermore, oral KS appears to be more aggressive and malignant than those occur on other sites such as the skin. Oral KS patients have a less than 10% 5-year survival rate (2).

Kaposi's sarcoma-associated herpesvirus (KSHV), also termed human herpesvirus type 8 (HHV-8), has been established to be an etiologic agent of KS (3). Additionally KSHV is also associated with two lymphoproliferative diseases, namely primary effusion lymphoma (PEL) and multicentric Castleman's disease (MCD) (1, 4, 5). KSHV is considered as a sexually transmitted pathogen in United States and West Europe and the transmission is mainly observed in MSM (men having sex with men) (4). However, studies found that oral exposure to infectious saliva is a potential risk factor for the acquisition of KSHV among MSM (6). It was also shown that KSHV is shed in saliva of infected individuals regardless of their HIV-1 status and viral titer in oral cavity is higher than that in all other sites of the body (6, 7). Saliva transmission is also responsible for mother-to-child vertical transmission in endemic areas as it was reported that the group of mothers who were not shedding KSHV in breast milk did shed the virus in saliva (8). Therefore, oral transmission is the main route of KSHV transmission.

KS is a multifocal and oligoclonal malignancy. Tumors comprise proliferating spindle-shaped KS cells with abundant inflammatory infiltrate and abnormal neoangiogenesis. The origin of the spindle-shaped KS cells lineage remains elusive. Based on initial immunohistochemistry studies as well as gene expression profiling research, the most widely accepted theory is that KS cells may derive from the endothelial cell lineage (9). KS cells express panendothelial markers (CD31, CD34 and Factor VIII) and lymphatic endothelial markers (VEGFR3, LYVE1 and PDPN). However, KS cells are poorly differentiated and also express other markers such as smooth muscle, dendritic cell and macrophage markers, indicating that KS cells do not faithfully represent endothelial cell lineage (10). The remarkable heterogeneity raised a possibility that KS may derive from mesenchymal stem cells or precursors of vascular cells (11, 12). This hypothesis appears to be plausible but has not yet been proven.

MSCs are characterized as a population of hierarchical postnatal stem cells with the potential to self-renew and differentiate into osteoblasts, chondrocytes, adipocytes, cardiomyocytes, myoblasts and neural cells (13, 14). Previous studies demonstrated that rat mesenchymal progenitor cells and human MSCs of bone marrow and other origins are susceptible to KSHV infection (11, 15, 16). The oral cavity contains a variety of distinctive MSC populations, including dental pulp stem cells (DPSCs), periodontal ligament stem cells (PDLSCs), apical papilla stem cells, dental follicle stem cells, and gingiva/mucosa-derived mesenchymal stem cells (GMSCs)(17–19). These MSCs of craniofacial tissues are mainly derived from cranial neural crest (20–22). Among them, MSCs in gingiva (GMSC) and in periodontal ligaments (PDLSCs) have potential to directly interact with oral cavity saliva, microbiota, and virus and have a chance to be infected by KSHV. In this study, we investigated the susceptibility of oral MSCs to KSHV infection and potential of infected MSCs to become KS cancer cells. We also searched for clinical evidences that support the view that KS spindle cells may originate from virally infected oral MSCs. Our

immunohistochemical studies of five AIDS-associated KS lesions revealed the presence of Nestin, a predominant marker for neural crest-derived precursor and MSCs, and CD29, a MSC marker known to be expressed in oral MSCs, in KS spindle cells, providing evidence for oral MSCs being a potential origin of KS cells. We showed that oral MSCs can be efficiently infected by KSHV and the infection promotes MSC differentiation that leads to morphological changes and enhanced capacities of adipogenesis, osteogenesis and angiogenesis. A transcription profiling study revealed that KSHV infection reprograms oral MSCs and transforms them to gain KS pathogenic features, indicating that mesenchymal-to-endothelial transition (MEndT) driven by KSHV infection contributes to the development of KS.

Materials and Methods

Ethic statements

The human sample collection and the use of PBMCs and PDLSCs in our research were approved the Medical Ethics Review Board of Sun Yet-sen University (Approval No. 2015-028). Written informed consent was provided by study participants. The animal experiments in this study were approved by Animal Ethics Review Board of Sun Yet-sen University (Approval No. 2015-041) and carried out strictly following the Guidance suggestion of caring laboratory animals, published by the Ministry of Science and Technology of the People's Republic of China.

Isolation of human PDLSCs, GMSCs and DPSCs and cell culture

Normal human impacted third molars and gingival tissue were collected from patients (12–25 years of age). The periodontal ligament tissues were scraped from third molars, and pulp tissue was gently separated from the crown and root. Gingival and dental pulp tissues were minced into 1- to 3-mm^2 fragments, and then digested at 37°C for 1.5 h in sterile PBS containing 3 mg/ml collagenase IV (Worthington Biochemical) and 4 mg/ml of dispase (Worthington Biochemical). Single-cell suspensions were obtained by passing the cells through a 70-μm strainer (Falcon), and then plated on 100 mm culture dishes (Corning) with complete α-MEM containing 10% FBS (BD Clontech), 100 U/ml penicillin/100 μg/ml streptomycin, 2 mM l-glutamine, 100 mM nonessential amino acid, and 550 μM 2-ME. Cells were cultured at 37°C with 5% CO_2. After 48 h, the nonadherent cells were removed. The plastic-adherent confluent cells were passaged with 0.05% trypsin containing 1 mM EDTA and continuously subcultured and maintained in the complete growth medium. Cells from the second to sixth passages were used in the experiments. Flow cytometric analysis was performed to confirm MSC surface markers. PDLSCs from five individuals were pooled for experiments to offset individual differences. Human Dermal Lymphatic Endothelial Cell (LEC) was purchased from ScienCell Research Laboratories, Inc (Cat. No. 2010), and cultured in Endothelial Cell Medium (ECM, ScienCell, Cat. No. 1001) containing 5% FBS, 1% Endothelial cell growth supplement (ECGS, ScienCell, Cat. No. 1052).

Reagents and antibodies

Cell culture medium α-MEM, penicillin and streptomycin were obtained from Invitrogen. Glutamine, nonessential amino acids, 2-ME, β-glycerophosphate dexamethasone, Alizarin

Red S, isobutylmethylxanthine, indomethacin, hydrocortisone, insulin, L-ascorbic acid phosphate, Oil Red O, Drabkin's reagent and paraformaldehyde were purchased from Sigma-Aldrich. L-ascorbic acid phosphate was from Wako and TRIzol reagent was from Invitrogen. Matrigel for tube assay was obtained from Corning. Antibodies against human CD29, CD73, CD90, CD105 and CD166 were purchased from BioLegend. PE-conjugated anti-human CD31, CD34, CD44, CD90, CD105 and CD166 were ordered form eBioscience. Anti-LANA (F0904) antibody was purchased from Advanced Biotechnologies, Inc. Anti-ETAR (EDNRA, sc-135902), anti-Vimentin (sc-6260), anti-PDPN (sc-376695) antibodies were purchased from Santa Cruz Biotechnology, Inc. Anti-Collagen I (ab292), anti-FGFR1 (ab137781) and anti-NRP1 (ab81321) were purchased from Abcam. Anti-PROX1 (BA2390) was purchased from Boster, China. Anti-NES (A0484), Anti-ITGB1 (CD29, A11060), Anti-ACTA2 (α-SMA, A7248), anti-VCAM1 (A0279) and anti-PML (A1184) was purchased from ABclonal Biotech Co. Ltd.

KSHV preparation and infection

iSLK.219 cells harboring rKSHV.219 were used for virus preparation. The cells were treated with 1μg/ml doxycycline and 1mM sodium butyrate and harvested 5 days post-induction. The culture supernatants were filtered through a 0.45-μm filter and centrifuged at 100000 g for 1 h. Pellet was resuspended in 1/100 volume of 1×PBS and stored at −80°C until use. Virus infection was performed according to established procedure. In brief, PDLSCs or LECs were seeded at 2×10^5 cell per well in 6-well plates, mixed with KSHV at MOI of 50 (viral genome equivalent) in the presence or absence of polybrene (5μg/ml). After centrifugation at 2,500 rpm for 60 min in room temperature, the cells were incubated at 37°C with 5% CO_2 for 2 h. Then the inoculum was removed by changing culture medium.

Immunofluorescence assay (IFA)

After washing with 1×PBS, KSHV-infected MSCs were fixed with 3.6% formaldehyde in PBS for 10 min, permeabilized in 0.1% Triton X-100 for 15 min, and blocked in 1% BSA for 1 h. Then the cells were incubated with antibodies against LANA (1:200 dilution), Vimentin (1:50 dilution), PDPN (1:50 dilution), EDNRA (1:50 dilution), FGFR1 (1:100 dilution) or α-SMA (1:100 dilution), respectively, for 1 h. Fluor Alexa-555-conjugated anti-IgG (Life technologies, 1:500 dilution) was used as secondary antibody. Slides were examined with a Zeiss LSM780 confocal laser scanning system (63×oil) and two channels were recorded sequentially.

Flow cytometry analysis

For quantitation of GFP-positive cells, PDLSCs, GMSCs, and DPSCs infected with KSHV were detached with 0.05% trypsin for 3~5 minutes, washed twice with PBS and centrifuged at 1500 rpm for 5 min. Cells were resuspended with PBS (containing 0.1% FBS) and quantified by flow cytometry analyzer (BD LSRFortessa). For analyses of cell surface markers, cells were digested, washed and resuspended as described above. Then cells were incubated with the following antibodies in 1:50 dilution: FITC-conjuncted antibodies against human CD29, CD73, CD90, CD105 and CD166, and PE-conjuncted anti-human CD31, CD34, CD44, CD90, CD105 and CD166. After 1 h incubation in room temperature, cells were washed twice with PBS and analyzed as described above.

Cell invasion assay

Cell invasion assays were carried out in 24-well Transwell units (Millipore). Briefly, polycarbonate filters with 8-μm pores were coated with 60 μl of matrigel-gel. PDLSCs or KSHV-PDLSCs (15,000 cells) in serum-free media were placed in the upper wells and the lower chambers were filled with 10% FBS medium. After 24 h incubation the cells that had passed through the filter were stained with crystal violet. The number of migrated cells was counted from multiple randomly selected microscopic visual fields using ImageJ software. Photographs were obtained and independent experiments were performed in triplicate.

ELISA

Media from mock-infected and KSHV-infected PDLSCs and LECs were harvested and centrifuged in 10000 rpm for 10 min. Cytokines in the media were determined using specific ELISA kits. ELISA kits for human IGF1 (Cat No. DG100), FGF basic (Cat No. DF850) and VEGF-D (Cat No. DVED00) were purchased from R&D Systems. Human VEGF-A ELISA kit (Cat No. BMS277/2) was purchased from eBioscience. Human TGFβ3 ELISA kit (Cat No. KA4402) was purchased from Abnova. Human ANGPT2 ELISA kit (Cat No. DL-ANGPT2-Hu) was purchased from DLdevelop.

Western Blot

Cells were lysed on ice for 30 min in lysis buffer [50 mM Tris-HCl, pH 7.4, 150 mM NaCl, 1% NP-40, 1% Triton X-100, 1 mM sodium orthovanadate (Na_3VO_4), 20 mM sodium pyrophosphate, 100 mM sodium fluoride, 10% glycerol, protease inhibitor cocktail (1 tablet in 50 mL lysis buffer)] and then centrifuged in 12,000 rpm for 10 min. The supernatants were mixed with loading buffer and heated at 95°C for 10 min. The whole cell extracts of 50 μg protein was resolved on a 10% SDS-PAGE and transferred onto nitrocellulose membranes. The membranes were blocked in 5% non-fat milk in 1×PBS for 1 h, and then incubated in diluted primary antibodies overnight at 4°C. IRDye 680LT and 800CW goat anti-rabbit IgG, anti-mouse IgG or anti-rat IgG antibodies (LI-COR Biosciences) was used as secondary antibody. An Odyssey system (LI-COR) was used for detection of proteins of interest.

Assays for osteogenic and adipogenic differentiation of MSCs

PDLSC or KSHV-infected PDLSC were seeded into 6-well plates (Corning) and cultured in growth medium until the cells reached confluence. To induce osteogenic differentiation, the MSCs were cultured under osteogenic culture conditions, containing 2 mM β-glycerophosphate, 100 mM L-ascorbic acid phosphate, and 10 nM dexamethasone in culture medium. Four weeks post-induction, 1% Alizarin Red S staining was performed to detect matrix mineralization(23). To retain Alizarin Red S, images were analyzed and quantified using NIH ImageJ software with a 50% threshold by determining the area positive for dye staining expressed as a fraction of the total area. For adipogenic induction, 500 nM isobutylmethylxanthine, 60 mM indomethacin, 500 nM hydrocortisone, 10 mg/mL insulin, and 100 nM L-ascorbic acid phosphate were added to the growth medium. After 2–3 weeks, the induced cells were stained with Oil Red O. The positive cells were quantified under microscopy and are shown relative to the total cell count.

Tube formation assay

Forty-eight-well plates were coated with Matrigel (1:1 dilute with α-MEM without FBS, 100μl/well) and incubated at 37°C for 1h to allow gelation to occur and avoid bubble. PDLSCs or KSHV-infected PDLSCs were resuspended in the medium and added to the top of the gel with 200μl α-MEM without FBS. The cells were incubated at 37°C with 5% CO2 for 8 h and images of tube formation were captured using a ZEISS fluorescence microscope. The quantification of the tube was carried out using the ImageJ software to measure the total length of tube in the image. The average value was used for the histogram.

Matrigel plug assay

Female C57BL/6J mice at 4 to 6 weeks old were obtained from the Animal Center of Sun Yat-sen University. Five mice were used for each treatment group. Cells ($5–10 \times 10^6$) in 100–200 μl of medium were prepared and thoroughly mixed with 500 μl matrigels to total volume of 600–800 μl, and subsequently implanted to mice by inguinal injection. After seven days, the mice were sacrificed and matrigel plugs were removed, photographed and subsequently dissolved in 1 ml Dispase reagent for 16 h at 37 °C. After removal of debris by centrifugation, hemoglobin was quantified using Drabkin's reagent (Sigma-Aldrich).

Kidney capsule transplantation

Four million of MSCs were collected and cultured on gelfoam scaffold for 1 day in regular medium. The host mouse was weighed and anesthetized by strictly following the animal care guidelines. Kidneys were exposed through incision of the skin and muscle on the back of the host mouse. The kidney capsule was opened with the fine tip of No.5 forceps. The MSC/scaffold block was placed under the kidney capsule. Sutures were placed close to the muscular layer and capsule grafting products were harvested 28 days after transplantation.

Histological analyses

Immunohistochemistry of Kaposi's sarcoma clinical samples for LANA, Nestin, and CD29 was performed on paraffin-embedded tumors from five AIDS-associated KS patients. Sections were subjected to antigen retrieval by using 10mM sodium citrate (pH 6.0) buffer for 10 minutes with an electric pressure cooker. Then tissues were blocked in 3% hydrogen peroxide for 10 minutes to quench the endogenous peroxidase activity and probed with antibodies against LANA (1:100), Nestin (1:50) or anti-CD29 (1:100) overnight. The primary antibody binding was detected using a goat anti-rabbit HRP secondary antibody (Product # 31460) followed by colorimetric detection using metal enhanced DAB. Tissues were counterstained with hematoxylin and prepped for mounting.

MSCs transplants were fixed in 4% paraformaldehyde and decalcified with 10% EDTA (pH 7.4) followed by paraffin embedding. Paraffin sections (7 μm) were stained with hematoxylin and eosin (H&E) and Masson's trichrome. To perform immunofluorescent staining, the paraffin-embedded sections were incubated with primary antibody (1:200) at 4°C overnight with rabbit IgG as negative control, and then treated with Alexa Fluor 594-conjugated secondary antibody (1:200, Life technologies) for 30 min at room temperature. Slides were mounted with VECTASHIELD mounting medium (Vector Laboratories).

RNA sequencing

Mock-infected and KSHV-infected (48 and 96 hours) PDLSCs were lysed with TRIzol reagent and total RNA was extracted following the manufacturer manual. RNA purity was checked using Qubit 3.0 Flurometer (Life Technologies, CA, USA). For each sample, 2 μg RNA was used to generate sequencing libraries with NEBNext Ultra™ RNA Library Prep Kit for Illumina (#E7530L, NEB, USA), referring to the manufacturer's recommendations. Index codes were added to attribute sequences to each sample. The libraries were sequenced on an Illumina Hiseq 4000 platform and 150 bp paired-end reads were generated.

Data process

Raw data in fastq format were filtered to gain high quality reads. The short reads were aligned to human reference genome (version hg19/GRCh37) and KSHV reference genome (version CQ994935.1). The number of clean tags mapped to indicated gene was counted by RPKM (Reads per Kilo bases per Million reads). Corrected p-value (q-value) < 0.05 and | log2 (fold change) | > 1 were set as threshold for significantly different expression.

Data analysis

Data of KS signature was from ArrayExpress Database (Accession E-MEXP-66)(24). Data of HDMEC and KSHV-infected HDMEC was from GEO database (GSE1377)(25). Data of HMVEC and KSHV-infected HMVEC was from GEO database (GSE6489)(26). Data of MEndT induction of hAMSC was from GEO database (GSE28385)(27). Enrichment analysis was performed with Gene Ontology (GO) tools, and GO terms with p value < 0.05 was considered as significantly enriched gene sets. Classification of different functions was primarily from GO enrichment analysis for Biological Process and KEGG pathway, then genes in relevant terms were classified into indicated categories. Venn diagrams were drawn by Venny 2.0 online (http://bioinfogp.cnb.csic.es/tools/venny/index.html).

In order to compare the RNA-seq data of mock- and KSHV-infected PDLSCs with the microarray data of KS and endothelial cells, the genes identified as KS expression signature were picked and aligned by Ensemble Gene ID, respectively. Genes containing an RPKM value of 0 were discarded. As PDLSCs are highly similar with bone marrow derived MSC, PDLSC data were normalized with the data of MSC microarray (24). Firstly, each sample was setting to equal scale. Then, a correction efficient for each gene was calculated by dividing the mean value of MSC with the mean RPKM value of PDLSC. Last, the RPKM value of each gene in mock- and KSHV-infected PDLSCs was multiplied with the indicated correction efficient. Unsupervised clustering of samples (X-axis) and genes (Y-axis) were preformed with average linkage method and Euclidean distance metric, respectively. Linkage distance with KS was performed by calculating the Pearson correlation coefficient with KS, and then subtracted by 1. The comparison of mock- and KSHV-infected PDLSCs with induced MEndT of hAMSCs was performed in the same way. For principal component analysis, normalized data were firstly analyzed and identified through SPSS 13.0 and then the plot was drawn with the first two components.

Statistical analysis

All data were analyzed with SPSS 13.0 program. Two-tailed Student's t-test and Chi-square test were performed, and p values<0.05 were considered as significant.

Data availability

RNA-seq data used in this manuscript were available in NCBI GEO (Gene Expression Omnibus) database, accession: GSE92341.

Results

Detection of oral MSC-specific markers in KS spindle cells

To trace the origin of KS spindle cells, we examined clinical KS lesion samples for specific cell type markers. Intermediate filament protein Nestin (Neuroectodermal stem cell marker) predominantly expresses in neural crest-derived stem/progenitor cells and is a useful molecular tool to characterize tumors originating from neural crest and mesenchymal lineages (28, 29). Neural crest is a group of embryonic cells that are pinched off during the formation of the neural tube and become stem cells of mesenchyme. These stem cells with a neural crest origin persist into adulthood, especially within the craniofacial compartment. Since oral MSCs are derived from neural crest, expression of Nestin in KS cells could suggest a lineage connection between oral MSCs and KS. In addition, CD29, also known as integrin β1, expresses in oral MSCs and is commonly used as an MSC marker (30, 31). Paraffin-embedded sections of KS from five AIDS-KS patients were subjected to immunohistochemical analyses with anti-Nestin and anti-CD29 antibodies. All the cases showed typical KS feathers, including abundant vasculature development, infiltration of mononuclear cells and red blood cells, and spindle-shaped KS cells. The majority of the spindle cells expressed LANA, further confirming the diagnosis of KS. The immunohistochemical staining showed that the majority of KS spindle cells in all five cases expressed Nestin and CD29 (Fig. 1A) and two cases, one carried the sarcoma in the palate (case 1) while the other had lesions in the palm (case 2), were shown in Fig. 1B.

Furthermore, oral MSCs from periodontal ligament (PDLSC), dental pulp (DPSC) and gingiva (GMSC), along with lymphatic endothelial cells (LECs), were prepared and examined for their expression of Nestin using immunofluoresces assay (IFA). Results showed that all three types of oral MSCs express Nestin. In contrast, LECs do not express Nestin and KSHV infection did not induce Nestin expression in LECs (Fig. 1C). The expression of Nestin in KS spindle cells as well as oral MSCs provides evidence that KS may originate from oral MSCs, which prompted us to continue pursuing the question if virally modified MSCs could become KS cells or precursors to KS.

Human oral MSCs are highly susceptible to KSHV infection and support establishment of viral latency

Oral cavity is the major route of KSHV infection and exposure to infectious saliva is mainly responsible for the transmission of the virus. Furthermore, our immunohistochemical analysis of KS lesions raised a possibility that KS may arise from KSHV-infected oral MSCs. These notions compelled us to examine the susceptibility of oral MSCs to KSHV

infection. Oral MSCs (PDLSC, DPSC and GMSC) were infected with recombinant GFP-expressing KSHV (rKSHV.219). Infectivity for MSCs of each type was estimated with the rate of the cells converted to GFP-positive. Results showed that all three types of oral MSCs were efficiently infected by KSHV (Fig. 2A, left panel) with infectivity rates from 72% to 87% in the presence of polybrene (Supplementary Data, Fig. S1A) and around 60% in the absence of polybrene (Fig. S1B). The infection led to successful latency establishment as indicated by LANA staining detected in the vast majority of cells (Fig. 2A, right panel). The infection was found to be persistent as LANA expression were detected in the majority of infected cells after four weeks of culture without drug selection pressure (Supplementary Data, Fig. S2). These results are consistent with previous studies with mesenchymal stem cells from diverse origins (11, 16) and indicate that oral MSCs are highly susceptible to KSHV infection and support establishment of latent infection. These findings raise a possibility that oral MSCs could be the primary target cells for KSHV infection in oral cavity.

KSHV infection leads to morphological and stem property changes of oral MSCs

Microscopic examination of the oral MSCs prior to and post KSHV infection revealed KSHV infection-associated morphological changes. Oral MSCs of three origins (PDLSC, DPSC and GMSC) displayed similar morphology of fibroblast-like cells. However, in the KSHV infected cell pool, some cells underwent morphological changes and showed an elongated shape (Fig. 2B).

The effects of KSHV infection on the stem cell property of oral MSCs were examined on the mesenchymal stem cell surface markers of infected MSCs. Over ninety-eight percent of uninfected PDLSCs were detected positive for mesenchyme markers CD29, CD44, CD73, CD90, CD105 and CD166 and only 1.4% and 9.5% cells expressed vascular endothelial marker CD34 or CD31, respectively (Fig. 2C and D). Interestingly, the ratio of mesenchymal stem cell marker positive cells significantly decreased in the pool infected with KSHV as shown in a two-dimensional flow cytometric analysis with GFP as an indicator for KSHV infected cells, suggesting the KSHV infection led to the loss of MSC marker expression (Fig. 2C). With the decreases of mesenchyme markers (CD44, CD90, CD105 and CD166), the endothelial markers CD31 and CD34, which are expressed in Kaposi’s sarcoma spindle cells, were significantly increased in KSHV-infected oral MSCs (Fig. 2D), suggesting that KSHV infection promote differentiation of oral MSCs.

Infection of oral MSCs promotes multiple lineage differentiation

To confirm if KSHV infection indeed enhances differentiation of oral MSCs, we tested the potentials of KSHV-infected oral MSCs in different lineage differentiation. We first examined the effect of KSHV infection on the ability of oral MSCs to differentiate into osteoblasts. Mock- and KSHV-infected PDLSCs were grown in the induced medium MSCOIM for two weeks and the osteogenic differentiation was examined by staining with Alizarin red S, which indicates calcium deposition. The result, shown in Fig. 3A, demonstrated an enhanced calcium deposition in KSHV-infected PDLSCs in comparison to mock-infected cells. The adipogenic differentiation was also compared between mock- and

KSHV-infected PDLSCs. Virally infected cells formed more lipid droplets visualized by higher absorbance of Oil Red O staining in comparison to mock-infected cells (Fig. 3B).

KS is a vascular tumor and abnormal angiogenesis is the hallmark of the malignancy. Angiogenesis is a multi-step process involving endothelial cell activation, proliferation, differentiation, migration, and formation of vascular structure. We examined if KSHV infection of oral MSCs promotes endothelial lineage differentiation and contributes to KSHV-induced angiogenesis. An *in vitro* Matrigel tubulogenesis assay was used to assess the ability of KSHV-infected oral MSCs in formation of capillary-like tubules that representing the later stage of angiogenesis. As shown in Fig. 3C, KSHV infection of PDLSCs increased the tubule formation, while tight cell junction was not formed among mock-infected MSCs. This result is consistent with two previous reports (16, 32). The tubulogenic ability of KSHV-infected MSCs was also examined after long-time culture. Result showed that KSHV-infected PDLSCs still preserved the ability of invasion and potential of forming tubules on Matrigel four weeks post-infection (Supplementary Data, Fig. S3, A and B). In addition, long-term infected PDLSCs also exhibited enhanced cell invasiveness in comparison with mock-infected cells (Fig. S3, C and D). These results indicate that a differentiation from oral MSCs to endothelial lineage took place and was enhanced by KSHV infection.

KSHV infection confers oral MSCs angiogenic phenotypes *ex vivo* through mesenchymal-to-endothelial transition

To further characterize KSHV-enhanced endothelial differentiation of oral MSCs and angiogenesis, we employed a murine Matrigel plug assay to analyze KSHV-infected PDLSCs for their ability of differentiation and angiogenesis *ex vivo*. Mock- and KSHV-infected PDLSCs were mixed with Matrigel without any cytokines and implanted to C57BL/6 mice. At day 7, the matrigel plugs were stripped out and examined for new blood vessel formation. KSHV infection of PDLSCs led to visibly more blood vessel formation on the Matrigel plug, which was also quantitated by measuring the hemoglobin content (Fig. 3D). In addition, mock- and KSHV-infected PDLSCs were transplanted into immunocompromised mice under the kidney capsule. Proliferation of implanted MSCs with slit-like vascular spaces that contain erythrocytes was observed in virally infected cells, but much less vascular spaces were seen in mock-infected cell transplant (Fig. 4A and B). Hematoxylin and eosin stain showed spindle-shaped cells resembling to these seen in KS lesion. Immunohistofluorescence staining showed expression of LANA and vascular endothelial marker CD31 in KSHV-infected PDLSCs transplant, not in mock-infected cell transplant (Fig. 4C and D). Furthermore, expression of Nestin and CD29 were detected in the implantation of both mock- and KSHV-infected MSCs but CD31 and CD34 only in KSHV-infected MSC implantation (Supplementary Data, Fig. S4). KSHV-induced expression of CD31 and CD34 in the MSC implants suggests that mesenchymal-to-endothelial transition (MEndT) took place in KSHV-infected MSCs in animal.

Altered gene expression profile reveals cellular reprograming in KSHV-infected oral MSCs

The finding that KSHV infection enhances MSCs differentiation suggests that the infection is able to reprogram the cells. To elucidate how KSHV infection reprograms oral MSCs and

if such reprograming drives the infected cells toward KS phenotype, we compared the gene expression profiles of MSCs prior to and post KSHV infection by using a deep RNA sequencing (RNA-seq) approach. PDLSCs were infected with rKSHV.219 at an MOI of 50 (viral genomic DNA equivalent) for 48 and 96 hours. These two post-infection time points were chosen as that allows identifying the changes of gene expression profile directly caused by KSHV infection. Forty-eight hour post-infection represents the early stage of KSHV primary infection while in 96 hour post-infection latent cycle gene expression has been established. Total RNAs were purified from the mock-and KSHV-infected cells and subjected to an RNA-seq analysis (Supplementary Data, Fig. S5A). The RNA-seq reads were first mapped to the KSHV genome (GenBank ID: GQ994935.1). The result shows that latent genes (LANA, ORF71 and ORF72) and a selected group of lytic genes (PAN RNA, ORF57, ORF64, vIL-6 and RTA) expressed in 48 hour post-infection (KSHV-48), while the expression of most lytic genes decreased and the latent genes continued to rise at 96 hour post-infection (KSHV-96) (Supplementary Data, Fig. S5B). The viral gene expression profile in oral MSCs is consistent with that of endothelial cells primarily infected by KSHV (33, 34) as well as virally infected PBMCs (35).

The reads were then mapped to the human genome. The RPKM (Reads Per Kilobase of transcript per Million mapped reads) of KSHV-48 and KSHV-96 cells were compared with mock-infected cells, that revealed 862 differential expressed genes (DEGs) in KSHV-48 and 1023 DEGs in KSHV-96. The KSHV-96 DEGs were subjected to a Gene Ontology (GO) analysis for significant association of the DEGs with specific GO terms. The molecular functions and biology process terms with the most enrichment levels are shown in Supplementary Data (Fig. S6, A and D). In order to define the similarity and difference between MSCs and endothelial cells in cell reprograming upon KSHV infection, DEGs from KSHV-infected human dermal endothelial cells (HDMEC) (25) and KSHV-infected pulmonary microvascular endothelial cells (HMVEC) (26), were included in the GO enrichment analysis (Supplementary Data, Fig. S6, B and E, C and F).

KSHV infection of oral MSCs exhibits mixed phenotypes of inflammatory cell infiltration, inflammation and angiogenesis

Among the top enriched molecular function categories, “cytokine activity” is uniquely found in KSHV-infected PDLSCs (Supplementary Data, Fig. S6A). The DEGs of KSHV-infected PDLSCs pertinent to cytokines, chemokines and their receptors are listed in Fig. 5A. A large spectrum of chemokines were significantly up-regulated in KSHV-infected PDLSCs. Given that KS is considered as a cytokine disease with strong infiltration of monocytes, macrophages and lymphocytes, KSHV-infected MSCs resemble KS cells in this phenotype. Among the chemokines, CCL5, CCL8 and CXCL10 were reported to be up-regulated in KS versus normal skin cells (24). Furthermore, many cytokines and growth factors involving endothelial development, angiogenesis and KS cell growth (such as ANGPT4, ANGPTL1, ANGPTL4, VEGF-A, -C and -D) as well as their receptors (VEGFR1 and 3, EDNRA and EDNRB) are among the DEGs of KSHV-infected PDLSCs, suggesting that KSHV-infected MSCs share the angiogenesis, autocrine and paracrine growth regulations with KS cells (36–38). The cells from KS lesions of AIDS patients constitutively release several growth factors and cytokines including FGF family. Two members from the FGF family, namely FGF2

(bFGF) and FGF7 were found up-regulated in KSHV-infected PDLSCs, showing a similarity between KSHV-infected MSCs and KS in cytokine-mediated autocrine and paracrine regulation of cell growth. Other inflammatory cytokines such as IL-1α, IL-1β, IL-6 and IL-10 were also up-regulated in KSHV-infected PDLSCs (Fig. 5A).

To confirm the RNA-seq data on the cytokine network in KSHV-infected MSCs and determine if it is a unique feature of infected MSCs, several representative cytokines were analyzed using ELISA for their production upon KSHV infection in MSCs and endothelial cells (lymphatic endothelial cells or LECs). It has been known that the FGF family is strongly expressed in KS, which is 100-fold higher than endothelial cells(37). Our data show that MSCs secreted a high level of bFGF, which was further enhanced by 2.5-fold upon KSHV infection (Fig. 5B). This cytokine was also up-regulated in KSHV-infected LECs, but the levels were 10-fold lower than infected MSCs (Fig. 5B). VEGF-A, VEGF-D, IGF1 and TGFβ3, the cytokines that support endothelial cell growth and differentiation, were up-regulated by 3–6-fold upon KSHV infection in MSCs. Interestingly, the productions of these four cytokines did not significantly change in LECs after KSHV infection (Fig. 5B–F). ANGPT2, an endothelial angiogenesis factor, was shown to express in both MSCs and LECs. However its secretion was significantly enhanced upon KSHV infection in LECs but little in MSCs (Fig. 5G). All the ELISA results were consistent with the RNA-seq data. Taken together, KSHV-infected PDLSCs leads to production of a large spectrum of cytokines and chemokines, exhibiting a mixed phenotype of inflammatory cell infiltration, inflammation and angiogenesis, which is consistent with typical KS features.

KSHV-mediated mesenchymal-to-endothelial transition transforms oral MSCs to KS-like cells in gene expression profile

As KSHV infection is able to confer MSCs KS-associated phenotypes such as endothelial lineage commitment, angiogenesis and chemokine/cytokine production, we asked if the cell reprograming led by KSHV infection transforms MSCs toward KS cells. To this end, we analyzed gene expression profile of KSHV-infected PDLSCs and compared it with KS signature genes established through analyzing DEGs of KS biopsy samples versus normal skin (24). The expression of KS signature genes in mock- and KSHV-infected PDLSCs was examined using an unsupervised clustering analysis. Mock- and KSHV-infected LECs and BECs (31) were also included in the assay for comparisons. Clustering of cell samples (X-axis) and genes (Y-axis) were performed by hierarchical clustering with average linkage method and euclidean distance metric. The similarity of each cell samples to KS cells in KS signature gene expression were determined by linkage distance based on Pearson correlation coefficient. Results showed that KSHV-infected PDLSC is much closer than mock-infected cell to KS in the gene expression profile (Fig. 6A). The linkage distances of different cell samples to KS cells are illustrated in Fig. 6B, showing the closest distance of KSHV-infected PDLSC to KS and significant difference between mock- and KSHV-infected PDLSC in this regard. The reliability of the analysis with this method (with normalization) was verified by re-analyzing the data reported in Wang et al (24), which resulted in similar results as originally reported (Supplementary data, Fig. S7) (24). To our surprise, our analysis did not detect significant difference in statistics between mock- and KSHV-infected LECs and BECs in KS signature gene expression (Fig. 6B). To further confirm our results on

relationships between cell groups and KS, principal component analysis was performed with the same set of data. Result, shown in Fig. 6C, also demonstrated that KSHV infection brought about a greater change in PDLSC than those in endothelial cells in distance toward KS.

Next, we focused on the DEGs of KSHV-infected PDLSCs and compared them with KS signature genes (the DEGs of KS biopsy samples versus normal skin) (31). The comparison identified 111 DEGs of KSHV-infected PDLSC that are overlapped with KS expression signature ($p<0.05$, $|logFC|>1$) (Fig. 6D). Eighty of the 111 genes (72%) are consistently regulated in both KS and KSHV-infected PDLSCs in the same direction as shown in Supplementary Data (Table S1). Gene ontology analysis showed that many of these consistent genes are involved in endothelial development, angiogenesis, chemotaxis and inflammation. For example, PROX1 (Prospero homeobox 1) is a master regulator of endothelial lineage differentiation (39, 40). Its expression is up-regulated in KS and KSHV-infected MSCs, suggesting an endothelial differentiation occurred in both cell settings. Other mesenchymal-to-endothelial differentiation-related genes such as PDPN [podoplanin, a downstream gene of PROX1 involved in lymphatic endothelial differentiation (41–43)], EDNRA (endothelin receptor A), PML (Promyelocytic leukemia), PGF (placental growth factor) and TGFβ3 are up-regulated in the same pattern in KSHV-infected PDLSCs and KS lesions (Table S1). These genes are expressed at relatively low levels in uninfected MSCs and KSHV infection enhanced their expression dramatically. The gene expression profile of KSHV-infected PDLSCs suggests that KSHV infection promotes a mesenchymal-to-endothelial transition (MEndT) in infected MSCs.

To confirm if MEndT indeed occurred during the KSHV-mediated reprogram in MSCs, we compared the gene expression profiles of mock- and KSHV-infected PDLSCs with a published MEndT gene profile (27). Human amnionic membrane-derived MSCs (hAMSCs) were induced in endothelial growth medium and considered as an MSC MEndT model (39). Interestingly an unsupervised clustering showed that KSHV-infected PDLSC has the first-level of distance with MEndT-occurred hAMSC, indicating KSHV-infected PDLSCs is very similar with MEndT MSCs in gene expression profile (Supplementary Data, Fig. S8). DEGs of KSHV-infected PDLSCs were then compared with the MEndT DEGs. Ninety-one genes are consistently expressed in these two cell settings and about 1/3 of them (31 genes) involved in differentiation ($p<0.05$, $|logFC|>1$) (Supplementary Data, Table S2). Among these genes are endothelial differentiation regulators (PROX1, PDPN and EDNRA) and cytokines (FGF5, FGF7 and TGFβ3). Another group of genes, which are associated with mesenchymal property including α-SMA, CNN1 (Calponin 1), TAGLN (Transgellin), NBEA (Neurobeachin), and DDIT3 (DNA-damage-inducible transcript 3) were down-regulated in both cell settings, a typical sign of MEndT. Up-regulation of endothelial related genes and down-regulation of mesenchymal related genes were also observed in KS lesions, suggesting the key role of MEndT process in KS tumorigenesis. Taken together, our results confirmed that KSHV infection promotes MEndT in MSCs, which contributes to KS pathogenesis.

KSHV infection reprograms MSCs and endothelial cells in two differentiation directions

KSHV-infected endothelial cells including human dermal endothelial cells (HDMEC) (25), pulmonary microvascular endothelial cells (HMVEC) (26), lymphatic endothelial cells (LECs) and blood vascular endothelial cells (BECs) (24) were included in the gene expression profiling analysis for comparison. Interestingly, the expression of the genes that are altered in KSHV-infected MSCs and involved in endothelial differentiation, vessel development and angiogenesis (such as PROX1, EDNRA, PML and PGF), was found to be largely reversed or unchanged in KSHV-infected LECs vs. LECs (Table S1). This result raised a possibility that KSHV infection drives opposite biological processes in these two types of cells, i.e. MEndT (differentiation) in MSCs and endothelial-to-mesenchymal (EndMT) (dedifferentiation) in LECs.

The hypothesis that KSHV infection of MSCs and endothelial cells reprograms cells in the opposite differential directions was tested as follows. First, we analyzed the DEGs of endothelial cells of different lineages against KS expression signature (Fig. 6D). Gene ontology analysis showed that among the common DEGs between KS and KSHV-infected endothelial cells, many genes are involved in endothelial-to-mesenchymal dedifferentiation process (Supplementary Data, Table S3–6). For example, Neuropilin 1 (NRP1, a co-receptor of VEGF and FGF, known as an EndMT marker) was induced in KSHV-infected HMVEC and LECs.

Second, a three-way comparison was made among KS signature genes, DEGs of KSHV-infected MSCs and endothelial cells (including HDMEC, HMVEC, LEC and BEC) to reveal the trend of MSC and endothelial cell reprograming upon KSHV infection. In contrast to KSHV-infected MSCs where many genes relevant to MEndT (endothelial differentiation and angiogenesis) are up-regulated, KSHV infection of endothelial cells down-regulates most of the MEndT-related genes and activates other classes of genes that favor endothelial-to-mesenchymal transition (EndMT) (Fig. 6E). Among the KS signature genes expressed in KSHV-infected MSCs and KSHV-infected endothelial cells, 8 genes (10%) in KSHV-infected MSCs are related to MEndT, while only 2 (1.49%) genes in KSHV-infected endothelial cells are classified in MEndT category. Conversely, 2 genes (2.5%) in KSHV-infected MSCs and 11 genes (8.21%) in KSHV-infected endothelial cells are associated with EndMT (Fig. 6E). Particularly in KSHV-infected endothelial cells, with the down-regulation of MEndT relevant genes (such as PROX1, PML, PGF, TGFBR2 and FGF2), some genes known to be involved in EndMT (such as Notch signaling Hey1, hedgehog signaling S1004, TGF-β signaling TGFB1I1, VEGF and FGF receptor NRP1) are up-regulated, suggesting that a dedifferentiation process occurred in KSHV-infected endothelial cells (Supplementary Data, Tables S3–6). In addition, the gene ontology analyses of 80 KS signature genes in KSHV-infected MSCs and 134 KS signature genes in endothelial cells also support the two-direction reprograming in MSC and endothelial cells (Supplementary Data, Fig. S6 G and H).

Third, several representative genes for MEndT and EndMT were chosen and examined for their responsiveness to KSHV infection in MSCs (PDLSCs) and endothelial cells (LEC) by Western or IFA. As shown in Fig. 7A and C, MEndT relevant genes PROX1, PDPN, EDNRA, PML and VCAM1 (vascular cell adhesion molecule 1 or CD106) were up-

regulated in PDLSCs in response to KSHV infection, but down-regulated (PROX1) or remained unchanged (PDPN, EDNRA, PML and VCAM1) in KSHV-infected LECs. On other hands, Vimentin (VIM), α-SMA (two typical mesenchymal-related genes), EndMT signature genes NRP1 (Neuropilin 1, a co-receptor of VEGF/FGF, known as an EndMT marker) and COL1A1 (type I Collagen Alpha 1 Chain) were up-regulated in LECs but remained unchanged in PDLSCs upon KSHV infection (except COL1A1 that was down-regulated in KSHV-infected PDLSCs) (Fig. 7B and D). In conclusion, these data revealed that KSHV infection can reprograms undifferentiated MSCs and differentiated endothelial cells in two differentiation directions: MEndT (differentiation) in MSCs, and EndMT (dedifferentiation) in endothelial cells, of which both may lead to transformation into KS cells.

Discussion

KSHV is mainly shed in saliva of infected individuals and oral exposure to infectious saliva is the major risk factor for the acquisition of KSHV. Thus, oral transmission is the major route of KSHV infection (6, 7). However, little is known about the nature of the target cells of KSHV infection in oropharynx. It was reported that a subset of tonsillar B cells can be infected by KSHV (44), and establish latent infection under a noncytolytic control by CD4 T cells (45). Given that the primary target cells should be highly susceptible to infection but infectivity rate of B cells to KSHV infection is generally low, whether tonsillar B cells are the original target for KSHV infection in oropharynx is in question. Mesenchymal stem cells (MSCs) are present in any vascularized tissues in human body including oral and craniofacial tissues. It has been reported that KSHV can efficiently infect human MSCs of diverse origins (11, 16). The oral cavity contains a variety of distinctive MSC populations, including dental pulp stem cells (DPSCs), periodontal ligament stem cells (PDLSCs), apical papilla stem cells, dental follicle stem cells, and gingiva/mucosa-derived mesenchymal stem cells (GMSCs) (17–19, 46–48). These MSCs show significantly increased proliferation and self-renewal capacities compared to bone marrow MSCs, which may be associated with their neural crest origin (20, 22, 49, 50). In the current study, we characterized the susceptibility of different oral MSCs including PDLSCs, GMSCs and DPSCs and found that all three types of oral MSCs are permissive to KSHV infection with infectivity rates between 72 to 87%. Among them, the MSCs in gingiva and periodontal ligaments (GMSCs and PDLSCs) have potential to directly interact with oral cavity saliva, microbiota and viruses and thus could serve as primary target cells for KSHV infection in oral cavity.

KSHV infection may lead to development of Kaposi’s sarcoma and other malignancies. Interestingly, in AIDS-associated KS patients, majority of KS manifest with oral lesions (1). The nature and cellular origin of KS spindle-shaped cells remains contentious. The current models for KS cell lineage include that (i) KSHV infects lymphatic endothelial cells (LEC) and drives them dedifferentiation towards blood endothelial cell (BEC) phenotype (24); (ii) KSHV infects BECs and drives them differentiation towards LEC phenotype (24); (iii) KSHV infects circulating endothelial progenitor cells and drives differentiation of these cells towards the LEC phenotype (51); (iv) KSHV infects LEC and drives EndMT (52). However, KS cells are poorly differentiated and do not faithfully represent any endothelial lineage (9). The multifocal and oligoclonal nature of KS suggests that the tumor cells derive from a

KSHV-infected progenitor cell with proliferation and differentiation potentials and the infection drives differentiation of the progenitor cell to KS spindle cells. The findings that KS spindle cells expresses neural crest and MSC markers and KSHV effectively infects oral MSCs raises a question whether virally modified MSCs could be possibly the origin of KS spindle cells. The proliferation and self-renewal nature of MSCs and the observation that KSHV infection of oral MSCs promoted cell multi-lineage differentiation completely support the hypothesis that KS could derive from KSHV-infected neural crest-derived MSCs.

The transformation of a progenitor cell, such as a KSHV-infected MSC, to a KS malignant cell needs a mesenchymal-to-endothelial transition (MEndT) process. A previous histogenetic study of clinical KS specimens has provided some evidence for MEndT in KS (12). KS lesions were shown to be positive of CD105, CD34, COX-2, VEGF, a-SMA and c-Kit, suggesting that KS originates from pluripotent MSCs and cannot be simply considered a pure vascular tumor (12). Although the observation provided a case-based hypothesis that KS spindle cells may originate from MSCs through MEndT, but could not definitively rule out the possibility that KS may arise from differentiated endothelial cells through endothelial-to-mesenchymal transition (EndMT). Our current study demonstrated that all of the five AIDS-KS lesions we tested express Neuroectodermal stem cell marker (Nestin) and oral MSC marker CD29, further arguing that at least in this five cases of AIDS-KS patients KS derived from neural crest-originated stem cells such as oral and craniofacial MSCs but unlikely from EndMT of terminally differentiated endothelial cells. Furthermore, our gene expression profiling study of KSHV-infected oral MSCs revealed how KSHV infection reprograms the infected MSCs and promotes MEndT, which includes activation of a number of genes that contribute to MEndT and express in KS lesions (24). Up-regulation of PROX1, PDPN and other MEndT promoting genes in both KSHV-infected MSCs and KS cells argues that the MEndT process occurs both in KSHV-infected MSCs and in KS development. The constant expression of PROX1 and PDPN in KS lesions renders the cancer cell the morphological and cellular characteristics of lymphatic endothelial lineage (39, 40), explaining why KS had been considered a neoplasm of lymphatic endothelium (53, 54). Taken together, our results provide both clinical and experimental evidence for KS spindle cells originating from neural crest-derived MSCs through MEndT, at least in AIDS-associated KS.

Interestingly, our analysis on KSHV-infected endothelial cells, which was originally included in our study as controls and references, demonstrated that KSHV infection can lead endothelial cells, especially terminally differentiated lymphatic endothelial cells (LECs), to an endothelial-to-mesenchymal transition (EndMT) process, opposite to the MEndT in KSHV-infected oral MSCs. In particular, PROX1 gene constantly expresses in LECs to maintain LEC identify, KSHV infection resulted in significant down-regulation of PROX1 expression. Additionally, KSHV infection also up-regulated a class of EndMT-related genes (such as vimentin, α-SMA, NRP1 and COL1A1) in LECs. Utilizing a 3D culture of KSHV-infected LEC, Cheng et al. (52) found that in 3D spheroids, KSHV infection induced transcriptional reprogramming of lymphatic endothelial cells to mesenchymal cells via EndMT. Taken together, these data suggest that KSHV infection apparently reprograms undifferentiated MSCs and terminally differentiated endothelial cells in two differentiation

directions: MEndT (differentiation) in MSCs, and EndMT (de-differentiation or trans-differentiation) in lymphatic endothelial cells. This notion let us further propose that KS spindle cells can arise from either KSHV-infected MSCs through a MEndT or from KSHV-infected LECs through an EndMT. How a virus can promote differentiation in MSCs and drive de-differentiation in LECs, reaching a same destination – KS cancer cells, warrants further investigation.

Finally, KSHV-infected oral MSCs closely resemble KS spindle cells in many pathogenic features of KS cells. KS is considered as a cytokine disease and abundant inflammatory infiltration is a pathogenic feature of KS (36, 37). In the early stage, KS is not a real sarcoma but an angiohyperplastic-inflammatory lesion mediated by inflammatory cytokines and angiogenic factors (36). KSHV infection of oral MSCs enhances the expression of a large number of chemokines (CCL5, CCL8, CXCL10, etc.), inflammatory cytokines (IL1, IL6, TNFSF10, etc) and angiogenic factors (bFGF, VEGF, PGF, ANGPTL2, etc.), of which many have been shown to be produced by KS, indicating the remarkable similarity between KSHV-infected MSCs and KS. Furthermore, KS is a vascular tumor and abnormal vascular space with red blood cells is another special feature of the lesion. We showed that KSHV infection of oral MSCs promotes blood vessel formation *in vitro*, *ex vivo* and in a mouse kidney capsule model, suggesting that KSHV infection can drive oral MSC into endothelial lineage differentiation and promote neoangiogenesis. Taken together, our results strongly suggest that KSHV-infected oral MSCs can be the progenitor of KS malignant cells and mesenchymal-to-endothelial transition driven by KSHV infection contributes to the development of KS.

Supplementary Material

Refer to Web version on PubMed Central for supplementary material.

Acknowledgments

We thank all members of the Yuan Lab for critical reading of the manuscript and helpful discussion. We are grateful to Dr. Ke Lan at Shanghai Institute Pasteur, Chinese Academy of Sciences for reagents and helps.

Financial Support: This work is supported by a NIH grant P01CA174439 (YY), National Natural Science Foundation of China grants 81530069 (YY), 81371793 (YW), the Guangdong Innovative Research Team Program (No. 2009010058).

References

1. Antman K, Chang Y. Kaposi’s sarcoma. The New England journal of medicine. 2000; 342:1027–38. [PubMed: 10749966]
2. Payne SF, Lemp GF, Rutherford GW. Survival following diagnosis of Kaposi’s sarcoma for AIDS patients in San Francisco. Journal of acquired immune deficiency syndromes. 1990; 3(Suppl 1):S14–7. [PubMed: 2395080]
3. Chang Y, Cesarman E, Pessin MS, Lee F, Culpepper J, Knowles DM, et al. Identification of herpesvirus-like DNA sequences in AIDS-associated Kaposi’s sarcoma. Science. 1994; 266:1865–9. [PubMed: 7997879]
4. Martin JN, Ganem DE, Osmond DH, Page-Shafer KA, Macrae D, Kedes DH. Sexual transmission and the natural history of human herpesvirus 8 infection. The New England journal of medicine. 1998; 338:948–54. [PubMed: 9521982]

5. Giffin L, Damania B. KSHV: pathways to tumorigenesis and persistent infection. Advances in virus research. 2014; 88:111–59. [PubMed: 24373311]
6. Pauk J, Huang ML, Brodie SJ, Wald A, Koelle DM, Schacker T, et al. Mucosal shedding of human herpesvirus 8 in men. The New England journal of medicine. 2000; 343:1369–77. [PubMed: 11070101]
7. Brayfield BP, Kankasa C, West JT, Muyanga J, Bhat G, Klaskala W, et al. Distribution of Kaposi sarcoma-associated herpesvirus/human herpesvirus 8 in maternal saliva and breast milk in Zambia: implications for transmission. The Journal of infectious diseases. 2004; 189:2260–70. [PubMed: 15181574]
8. Minhas V, Wood C. Epidemiology and transmission of Kaposi's sarcoma-associated herpesvirus. Viruses. 2014; 6:4178–94. [PubMed: 25375883]
9. Cancian L, Hansen A, Boshoff C. Cellular origin of Kaposi's sarcoma and Kaposi's sarcoma-associated herpesvirus-induced cell reprogramming. Trends in cell biology. 2013; 23:421–32. [PubMed: 23685018]
10. Mesri EA, Cesarman E, Boshoff C. Kaposi's sarcoma and its associated herpesvirus. Nature reviews Cancer. 2010; 10:707–19. [PubMed: 20865011]
11. Jones T, Ye F, Bedolla R, Huang Y, Meng J, Qian L, et al. Direct and efficient cellular transformation of primary rat mesenchymal precursor cells by KSHV. The Journal of clinical investigation. 2012; 122:1076–81. [PubMed: 22293176]
12. Gurzu S, Ciortea D, Munteanu T, Kezdi-Zaharia I, Jung I. Mesenchymal-to-endothelial transition in Kaposi sarcoma: a histogenetic hypothesis based on a case series and literature review. PloS one. 2013; 8:e71530. [PubMed: 23936513]
13. Friedenstein AJ, Chailakhyan RK, Latsinik NV, Panasyuk AF, Keiliss-Borok IV. Stromal cells responsible for transferring the microenvironment of the hemopoietic tissues. Cloning in vitro and retransplantation in vivo. Transplantation. 1974; 17:331–40. [PubMed: 4150881]
14. Prockop DJ. Marrow stromal cells as stem cells for nonhematopoietic tissues. Science. 1997; 276:71–4. [PubMed: 9082988]
15. Parsons CH, Szomju B, Kedes DH. Susceptibility of human fetal mesenchymal stem cells to Kaposi sarcoma-associated herpesvirus. Blood. 2004; 104:2736–8. [PubMed: 15238422]
16. Lee MS, Yuan H, Jeon H, Zhu Y, Yoo S, Shi S, et al. Human Mesenchymal Stem Cells of Diverse Origins Support Persistent Infection with Kaposi's Sarcoma-Associated Herpesvirus and Manifest Distinct Angiogenic, Invasive, and Transforming Phenotypes. mBio. 2016; 7:e02109–15.
17. Gronthos S, Mankani M, Brahim J, Robey PG, Shi S. Postnatal human dental pulp stem cells (DPSCs) in vitro and in vivo. Proceedings of the National Academy of Sciences of the United States of America. 2000; 97:13625–30. [PubMed: 11087820]
18. Miura M, Gronthos S, Zhao M, Lu B, Fisher LW, Robey PG, et al. SHED: stem cells from human exfoliated deciduous teeth. Proceedings of the National Academy of Sciences of the United States of America. 2003; 100:5807–12. [PubMed: 12716973]
19. Morsczeck C, Gotz W, Schierholz J, Zeilhofer F, Kuhn U, Mohl C, et al. Isolation of precursor cells (PCs) from human dental follicle of wisdom teeth. Matrix biology: journal of the International Society for Matrix Biology. 2005; 24:155–65. [PubMed: 15890265]
20. Chai Y, Jiang X, Ito Y, Bringas P Jr, Han J, Rowitch DH, et al. Fate of the mammalian cranial neural crest during tooth and mandibular morphogenesis. Development. 2000; 127:1671–9. [PubMed: 10725243]
21. Ibarretxe G, Crende O, Aurrekoetxea M, Garcia-Murga V, Etxaniz J, Unda F. Neural crest stem cells from dental tissues: a new hope for dental and neural regeneration. Stem cells international. 2012:103503. [PubMed: 23093977]
22. Xu X, Chen C, Akiyama K, Chai Y, Le AD, Wang Z, et al. Gingivae contain neural-crest- and mesoderm-derived mesenchymal stem cells. Journal of dental research. 2013; 92:825–32. [PubMed: 23867762]
23. Chen X, He F, Zhong DY, Luo ZP. Acoustic-frequency vibratory stimulation regulates the balance between osteogenesis and adipogenesis of human bone marrow-derived mesenchymal stem cells. BioMed research international. 2015; 2015:540731. [PubMed: 25738155]

24. Wang HW, Trotter MW, Lagos D, Bourboulia D, Henderson S, Makinen T, et al. Kaposi sarcoma herpesvirus-induced cellular reprogramming contributes to the lymphatic endothelial gene expression in Kaposi sarcoma. Nature genetics. 2004; 36:687–93. [PubMed: 15220918]
25. Hong YK, Foreman K, Shin JW, Hirakawa S, Curry CL, Sage DR, et al. Lymphatic reprogramming of blood vascular endothelium by Kaposi sarcoma-associated herpesvirus. Nature genetics. 2004; 36:683–5. [PubMed: 15220917]
26. Bull TM, Meadows CA, Coldren CD, Moore M, Sotto-Santiago SM, Nana-Sinkam SP, et al. Human herpesvirus-8 infection of primary pulmonary microvascular endothelial cells. American journal of respiratory cell and molecular biology. 2008; 39:706–16. [PubMed: 18587055]
27. Konig J, Huppertz B, Desoye G, Parolini O, Frohlich JD, Weiss G, et al. Amnion-derived mesenchymal stromal cells show angiogenic properties but resist differentiation into mature endothelial cells. Stem Cells Dev. 2012; 21:1309–20. [PubMed: 21762016]
28. Xie L, Zeng X, Hu J, Chen Q. Characterization of Nestin, a Selective Marker for Bone Marrow Derived Mesenchymal Stem Cells. Stem Cells Int. 2015; 2015:762098. [PubMed: 26236348]
29. Lobo MV, Arenas MI, Alonso FJ, Gomez G, Bazan E, Paino CL, et al. Nestin, a neuroectodermal stem cell marker molecule, is expressed in Leydig cells of the human testis and in some specific cell types from human testicular tumours. Cell Tissue Res. 2004; 316:369–76. [PubMed: 15127288]
30. Kawashima N. Characterisation of dental pulp stem cells: a new horizon for tissue regeneration? Arch Oral Biol. 2012; 57:1439–58. [PubMed: 22981360]
31. Pittenger MF, Mackay AM, Beck SC, Jaiswal RK, Douglas R, Mosca JD, et al. Multilineage potential of adult human mesenchymal stem cells. Science. 1999; 284:143–7. [PubMed: 10102814]
32. Yoo SM, Jang J, Yoo C, Lee MS. Kaposi's sarcoma-associated herpesvirus infection of human bone-marrow-derived mesenchymal stem cells and their angiogenic potential. Archives of virology. 2014; 159:2377–86. [PubMed: 24777829]
33. Gao SJ, Deng JH, Zhou FC. Productive lytic replication of a recombinant Kaposi's sarcoma-associated herpesvirus in efficient primary infection of primary human endothelial cells. Journal of virology. 2003; 77:9738–49. [PubMed: 12941882]
34. Yoo SM, Zhou FC, Ye FC, Pan HY, Gao SJ. Early and sustained expression of latent and host modulating genes in coordinated transcriptional program of KSHV productive primary infection of human primary endothelial cells. Virology. 2005; 343:47–64. [PubMed: 16154170]
35. Purushothaman P, Thakker S, Verma SC. Transcriptome analysis of Kaposi's sarcoma-associated herpesvirus during de novo primary infection of human B and endothelial cells. Journal of virology. 2015; 89:3093–111. [PubMed: 25552714]
36. Ensoli B, Sturzl M. Kaposi's sarcoma: a result of the interplay among inflammatory cytokines, angiogenic factors and viral agents. Cytokine & growth factor reviews. 1998; 9:63–83. [PubMed: 9720757]
37. Ensoli B, Nakamura S, Salahuddin SZ, Biberfeld P, Larsson L, Beaver B, et al. AIDS-Kaposi's sarcoma-derived cells express cytokines with autocrine and paracrine growth effects. Science. 1989; 243:223–6. [PubMed: 2643161]
38. Hu J, Jham BC, Ma T, Friedman ER, Ferreira L, Wright JM, et al. Angiopoietin-like 4: a novel molecular hallmark in oral Kaposi's sarcoma. Oral Oncol. 2011; 47:371–5. [PubMed: 21421336]
39. Hong YK, Harvey N, Noh YH, Schacht V, Hirakawa S, Detmar M, et al. Prox1 is a master control gene in the program specifying lymphatic endothelial cell fate. Developmental dynamics: an official publication of the American Association of Anatomists. 2002; 225:351–7. [PubMed: 12412020]
40. Johnson NC, Dillard ME, Baluk P, McDonald DM, Harvey NL, Frase SL, et al. Lymphatic endothelial cell identity is reversible and its maintenance requires Prox1 activity. Genes & development. 2008; 22:3282–91. [PubMed: 19056883]
41. Renart J, Carrasco-Ramirez P, Fernandez-Munoz B, Martin-Villar E, Montero L, Yurrita MM, et al. New insights into the role of podoplanin in epithelial-mesenchymal transition. International review of cell and molecular biology. 2015; 317:185–239. [PubMed: 26008786]

42. Fu J, Gerhardt H, McDaniel JM, Xia B, Liu X, Ivanciu L, et al. Endothelial cell O-glycan deficiency causes blood/lymphatic misconnections and consequent fatty liver disease in mice. The Journal of clinical investigation. 2008; 118:3725–37. [PubMed: 18924607]
43. Pan Y, Yago T, Fu J, Herzog B, McDaniel JM, Mehta-D'Souza P, et al. Podoplanin requires sialylated O-glycans for stable expression on lymphatic endothelial cells and for interaction with platelets. Blood. 2014; 124:3656–65. [PubMed: 25336627]
44. Hassman LM, Ellison TJ, Kedes DH. KSHV infects a subset of human tonsillar B cells, driving proliferation and plasmablast differentiation. The Journal of clinical investigation. 2011; 121:752–68. [PubMed: 21245574]
45. Myoung J, Ganem D. Generation of a doxycycline-inducible KSHV producer cell line of endothelial origin: maintenance of tight latency with efficient reactivation upon induction. Journal of virological methods. 2011; 174:12–21. [PubMed: 21419799]
46. Yazawa T, Kawabe S, Inaoka Y, Okada R, Mizutani T, Imamichi Y, et al. Differentiation of mesenchymal stem cells and embryonic stem cells into steroidogenic cells using steroidogenic factor-1 and liver receptor homolog-1. Molecular and cellular endocrinology. 2011; 336:127–32. [PubMed: 21129436]
47. Seo BM, Miura M, Gronthos S, Bartold PM, Batouli S, Brahim J, et al. Investigation of multipotent postnatal stem cells from human periodontal ligament. Lancet. 2004; 364:149–55. [PubMed: 15246727]
48. Zhang Q, Shi S, Liu Y, Uyanne J, Shi Y, Shi S, et al. Mesenchymal stem cells derived from human gingiva are capable of immunomodulatory functions and ameliorate inflammation-related tissue destruction in experimental colitis. Journal of immunology. 2009; 183:7787–98.
49. Driskell RR, Clavel C, Rendl M, Watt FM. Hair follicle dermal papilla cells at a glance. Journal of cell science. 2011; 124:1179–82. [PubMed: 21444748]
50. Chai Y, Maxson RE Jr. Recent advances in craniofacial morphogenesis. Developmental dynamics: an official publication of the American Association of Anatomists. 2006; 235:2353–75. [PubMed: 16680722]
51. Asahara T, Masuda H, Takahashi T, Kalka C, Pastore C, Silver M, et al. Bone marrow origin of endothelial progenitor cells responsible for postnatal vasculogenesis in physiological and pathological neovascularization. Circulation research. 1999; 85:221–8. [PubMed: 10436164]
52. Cheng F, Pekkonen P, Laurinavicius S, Sugiyama N, Henderson S, Gunther T, et al. KSHV-initiated notch activation leads to membrane-type-1 matrix metalloproteinase-dependent lymphatic endothelial-to-mesenchymal transition. Cell host & microbe. 2011; 10:577–90. [PubMed: 22177562]
53. Beckstead JH, Wood GS, Fletcher V. Evidence for the origin of Kaposi's sarcoma from lymphatic endothelium. The American journal of pathology. 1985; 119:294–300. [PubMed: 2986460]
54. Jussila L, Valtola R, Partanen TA, Salven P, Heikkila P, Matikainen MT, et al. Lymphatic endothelium and Kaposi's sarcoma spindle cells detected by antibodies against the vascular endothelial growth factor receptor-3. Cancer research. 1998; 58:1599–604. [PubMed: 9563467]

A

Case	KS Type	Age	Tumor Location	Expression of Markers		
				LANA	Nestin	CD29
1	AIDS-KS	31	Palate	+	+	+
2	AIDS-KS	30	Right Palm	+	+	+
3	AIDS-KS	24	Rectum	+	+	+
4	AIDS-KS	26	Cervical Lymph Node	+	+	+
5	AIDS-KS	61	Facial Skin	+	+	+

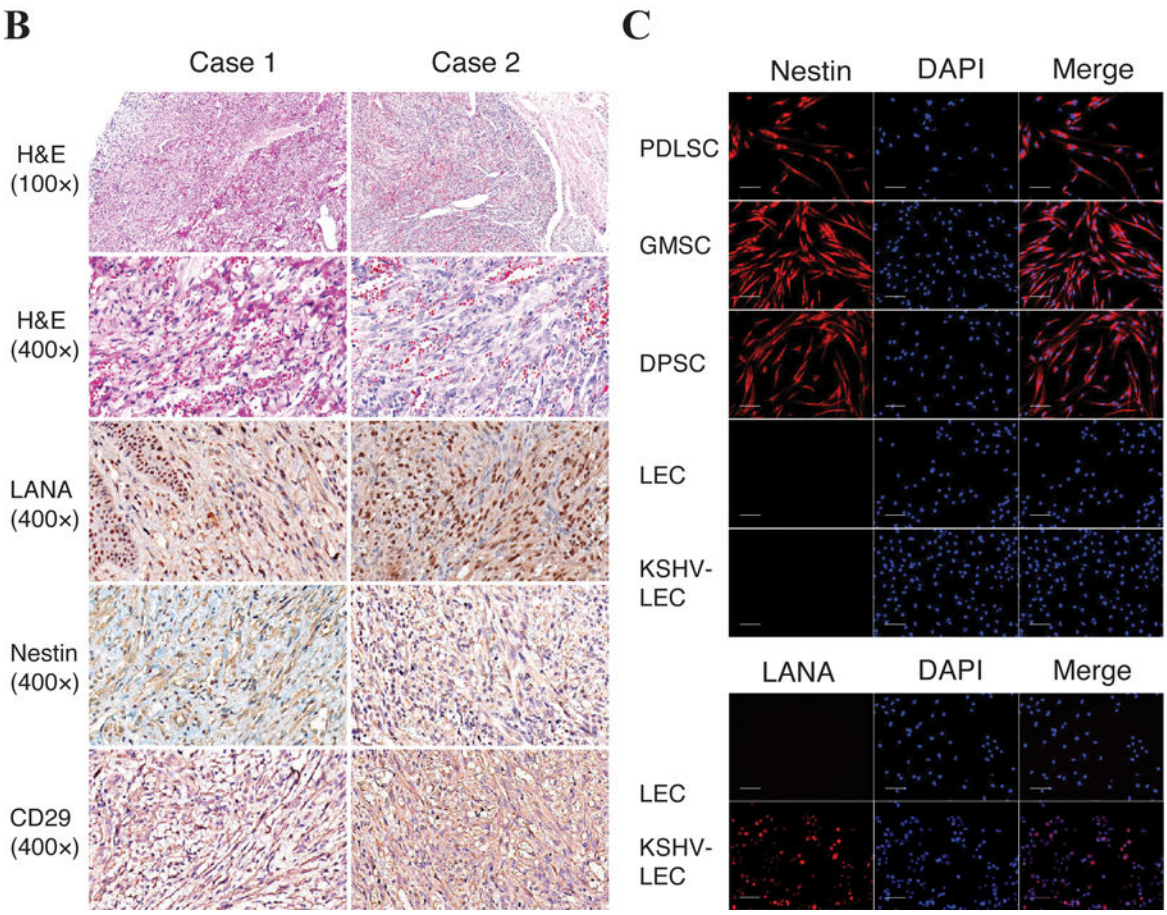

Fig. 1. AIDS-KS spindle cells exhibit oral MSC-specific markers

(A) Paraffin-embedded sections of KS lesions from five AIDS-KS patients were subjected to immunohistochemical analyses for LANA, Nestin and CD29. (B) Two cases, one carrying the sarcoma in the palate and the other in the palm, are illustrated. H&E staining reveals typical KS histological feathers such as spindle shaped KS cells and slit-like vascular channels with erythrocytes. Immunohistochemical staining shows LANA, Nestin and CD29 in KS spindle cells. (C) Oral MSCs from periodontal ligament (PDLSC), dental pulp (DPSC) and gingiva (GMSC), along with lymphatic endothelial cells (LECs) and KSHV-

infected LECs, were examined for their expression of Nestin using IFA and DAPI. KSHV infection of LECs was confirmed by IFA with an anti-LANA antibody.

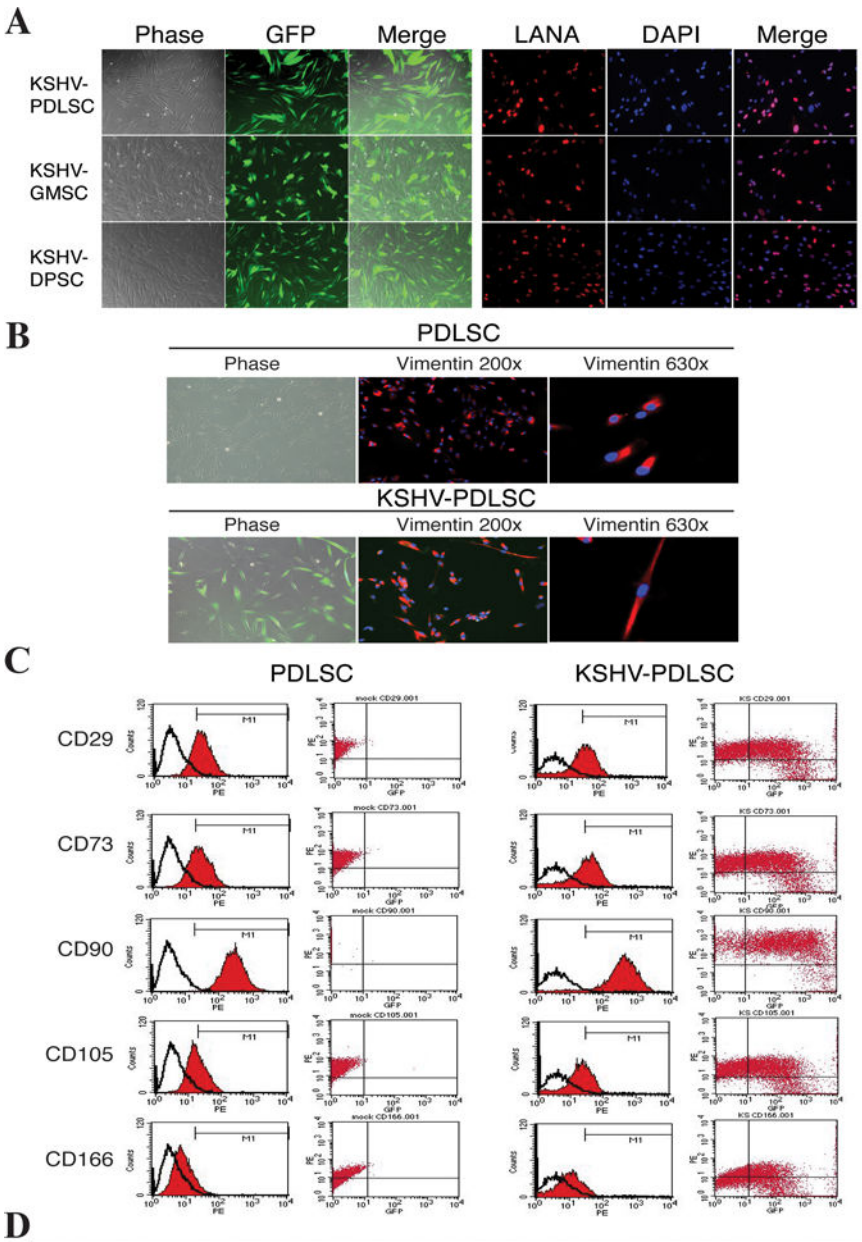

D

	CD31	CD34	CD44	CD90	CD105	CD166
PDLSC	9.5%	1.4%	98.8%	99.5%	98%	98.6%
KSHV-PDLSC	46.5%	18.1%	95.9%	89.4%	90.7%	85.7%

Fig. 2. Human oral MSCs are highly susceptible for KSHV infection and viral latent infection leads to morphological and cell marker changes of MSCs

(A) Primary oral MSCs of different origins (PDLSCs, GMSCs and DPSCs) were infected with GFP-KSHV in an MOI of 50 (KSHV genome equivalent) for 48 hours and analyzed by GFP fluoresces. (B) Infected cells were drug-selected for a week followed by two weeks culture without selection and analyzed by IFA with anti-Vimentin antibody. Images show the phase-contrast, the antibody staining and GFP fluorescence of the cells. (C) Flow cytometric analysis of mock- and KSHV-infected PDLSCs with mesenchyme markers (CD29, CD73,

CD90, VD105 and CD166, Y-axis) and GFP (KSHV-infected cells, X-axis). (D) The expression of mesenchymal and endothelial markers in mock- and KSHV-infected PDLSCs.

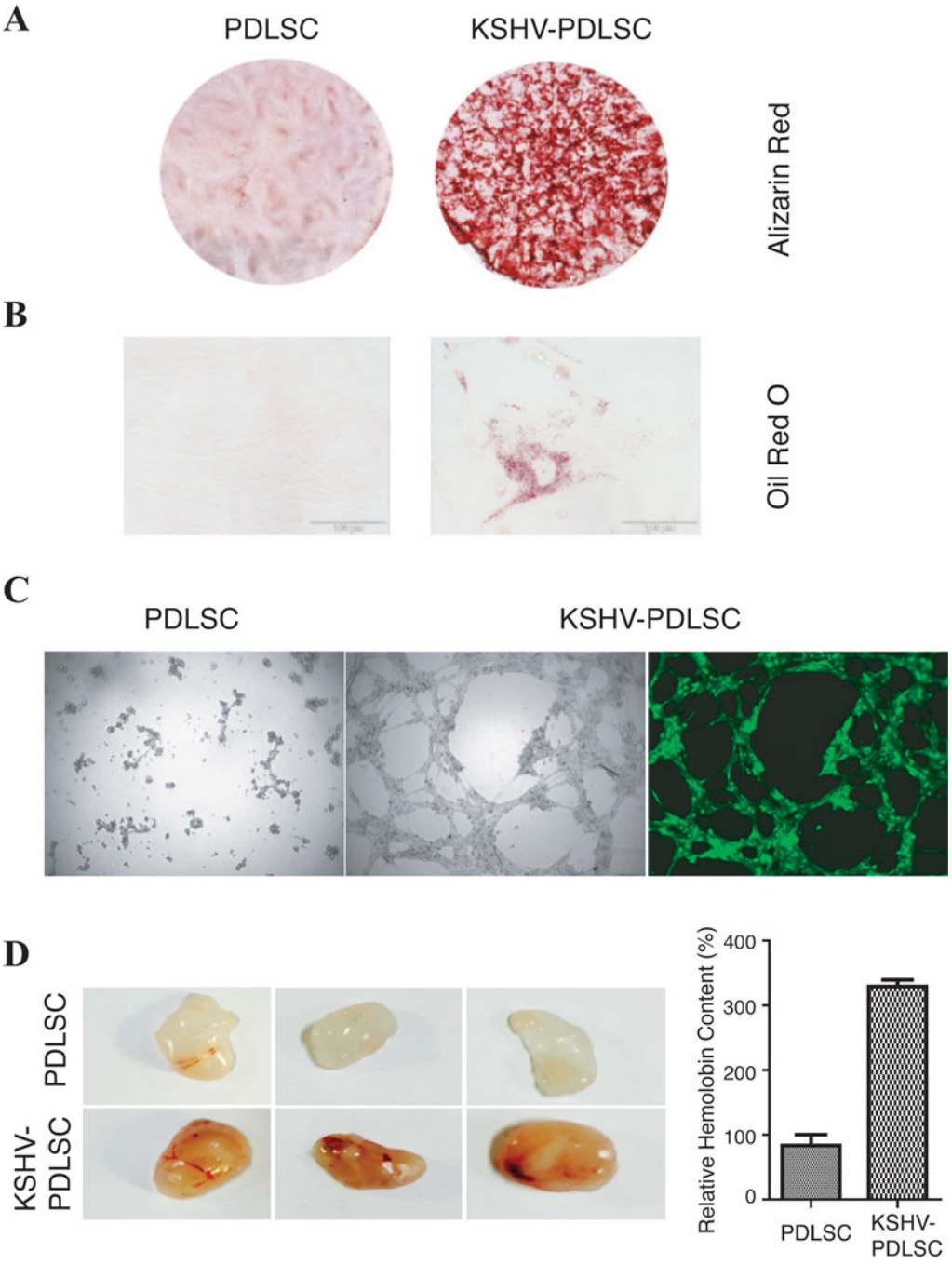

Fig. 3. KSHV infection promotes multi-lineage differentiation

PDLSCs were mock- and KSHV-infected in an MOI of 50 (viral genomic DNA equivalent). (A) Cells were induced under osteogenic culture condition for 4 weeks and assayed for their osteogenic differentiation by Alizarin staining. (B) PDLSCs were subjected to adipogenic induction and adipogenic differentiation was analyzed by oil Red staining. (C) Mock- and virally infected PDLSCs were loaded on the top of Matrigel and the ability of the cells in formation of capillary-like tubules was analyzed under a ZEISS fluorescence microscope. (D) The effect of KSHV infection on angiogenesis property of PDLSCs was also examined

ex vivo using the Matrigel plug assay. Matrigel containing mock- or KSHV-infected PDLSCs were subcutaneously implanted into C57BL/6 mice. After 7 days, Matrigel plug were removed and photographed. After Matrigel plugs were homogenized and centrifuged, their supernatant was used to quantitate the haemoglobin content using Drabkin's reagent.

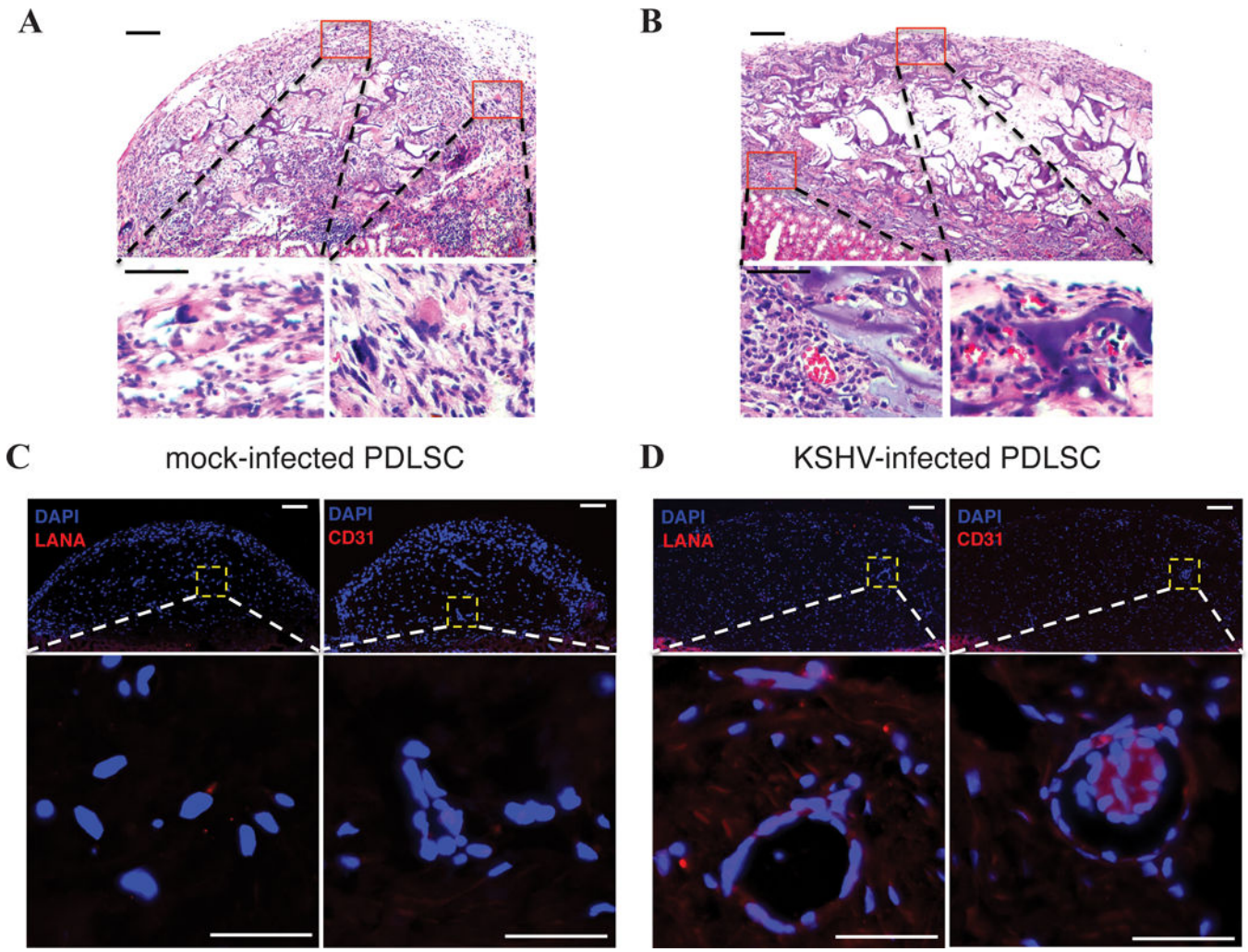

Fig. 4. Kidney capsule implantation of KSHV-infected MSCs

KSHV infected-PDLSCs (1×10^6 cells) were implanted into kidney capsule. Spindle-like cells, sieve-like pattern, and mononuclear cells, with slit-like vascular spaces containing red blood cells were observed (B in comparison to A). Immunohistofluorescence staining showed expression of LANA and vascular endothelial marker CD31 in KSHV-infected human PDLSC transplant (B in comparison to A). Bar: 50 μm.

A

Function cluster	KSHV-PDLSC vs. PDLSC				KSHV-HDMEC vs. HDMEC				KSHV-HMVEC vs. HMVEC			
	Cytokine	Change	Receptor	Change	Cytokine	Change	Receptor	Change	Cytokine	Change	Receptor	Change
Chemotaxis	CCL2	+	CCR1	+	CCL14	+			CCL14	+		
	CCL5	+			CCL15	+			CCL15	+		
	CCL7	+	CCR3	+	CCL23	+			CXCL5	+		
	CCL8	+			CXCL13	-	CXCR5	+	CXCL10	+		
	CCL13	+			CXCL18	-	CXCR6	+	CXCL11	+		
	CXCL1	+							CXCL12	-	CXCR4	+
	CXCL3	+							CXCL16	+		
	CXCL5	+										
	CXCL6	+										
	CXCL10	+										
	CXCL11	-	CXCR7	+								
	CXCL12	-										
	CXCL16	+										
Endothelial development & angiogenesis	ANGPT4	+			ANGPT2	+			ANGPT2	+		
	ANGPTL1	+			LEP	-	LEPR	+	ANGPTL2	+		
	ANGPTL2	+			EDN1	-	EDNRB	+				
	ANGPTL4	+			FGF12	+						
	ANGPTL5	+			FGF13	+						
	EDN1	-	EDNRA	+								
			EDNRB	+								
	FGF2(bFGF)	+										
	FGF7	+										
	FIGF(VEGFD)	+										
	PGF	+										
	VEGFA	+	VEGFR1	+								
	VEGFC		VEGFR3	+								
Inflammation	IL1α	+			IL1α	-	IL1R1	+	IL6	+		
	IL1β	+			IL1β	-			TNFSF4	+		
	IL6	+			IL3	-	IL3RA	+	TNFSF18	+		
	IL10	-	IL10R	+	IL5	+						
	TNFSF4	+			TNFα	+						
	TNFSF10	+			TNFSF1	+						
	TNFSF13B	+										
	TNFSF15	+										
Growth & differentiation	TGFβ3	+	TGFβR2	+	TGFα	+			PGF	+		
	OSM	+										
	IGF1	+										
	TSP1	-	CD36	+								
	INHBA	+										
	INHBB	+										

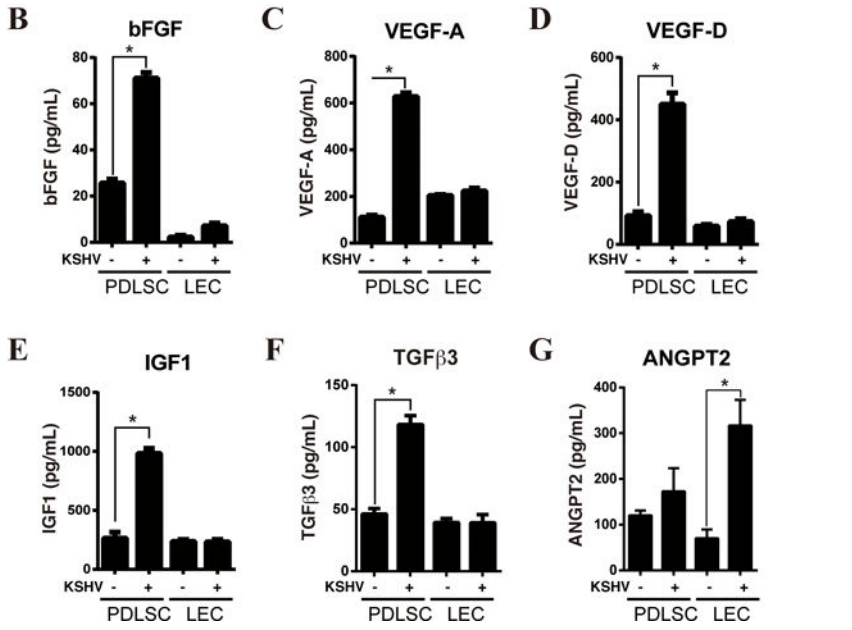

Fig. 5. Expression and secretion of chemokines and cytokines in PDLSCs and endothelial cells upon KSHV infection

(A) Chemokines and cyckines that are up-regulated in KSHV-infected PDLSCs identified in our RNA-seq analysis are listed. Genes that were reported to be over-expressed in KS lesions are marked in red. The cytokines that are up-regulated in HDMEC and HMVECs upon KSHV infection are included as comparison. (B-G) PDLSCs and LECs were infected with KSHV in a MOI of 50 (viral genomic DNA equivalent). The infectivity rates of PDLSCs and LECs were determined using GFP fluorescence and were 92.1% and 88.5% respectively. Ninety-six hours post-infection, mock- and KSHV-infected cells were seeded in

a relative low density (1×10^5 per mL) with α-MEM containing 1% FBS. Supernatants were collected after 6 hours, and subjected to ELISA for bFGF, VEGF-A and VEGF-D, IGF1, TGFβ3 and ANGPT2.

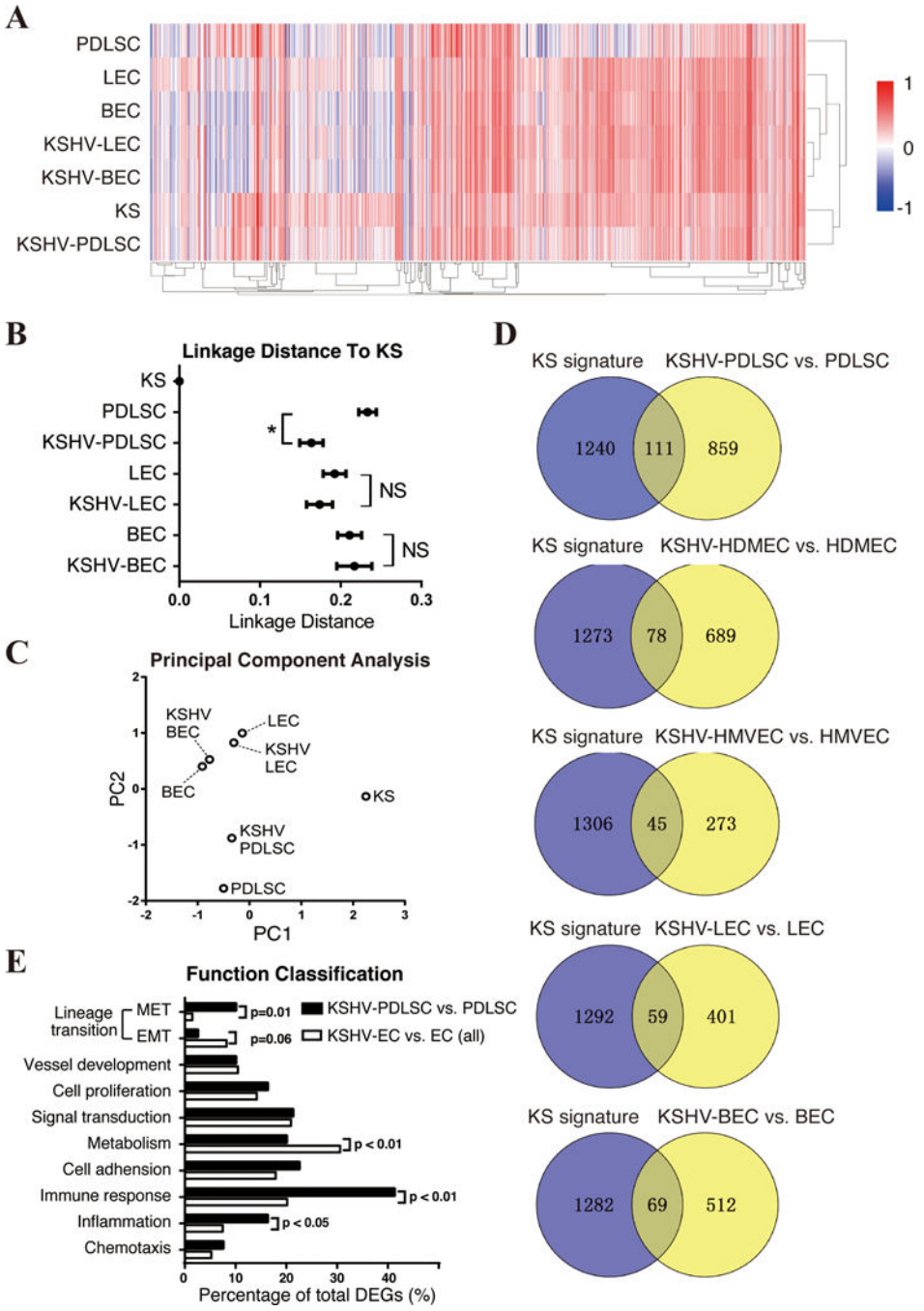

Fig. 6. Relationship of KSHV-infected MSCs and endothelial cells to KS in gene expression profile

(A) Genes listed in KS signature were picked from uninfected and KSHV-infected MSC, LEC and BEC, and shown by heatmap. RNA-seq Data of KSHV-PDLSC and PDLSC were normalized with the Microarray data of MSC (31). Unsupervised clustering of samples (X-axis) and genes (Y-axis) were performed by average linkage method. (B) Linkage distance between KS and each cell group was determined by Pearson correlation coefficient. (C) First two principal components of these data were identified and shown in multipledimensional scaling (MDS) plot. (D) DEGs from KSHV-infected MSCs and ECs are compared with KS

signature with venny diagram. (E) The genes that are consistently regulated in KS and KSHV-infected MSCs or ECs were assorted according to their functions, and compared respectively. “NS”, no significance. “*”, $p<0.05$.

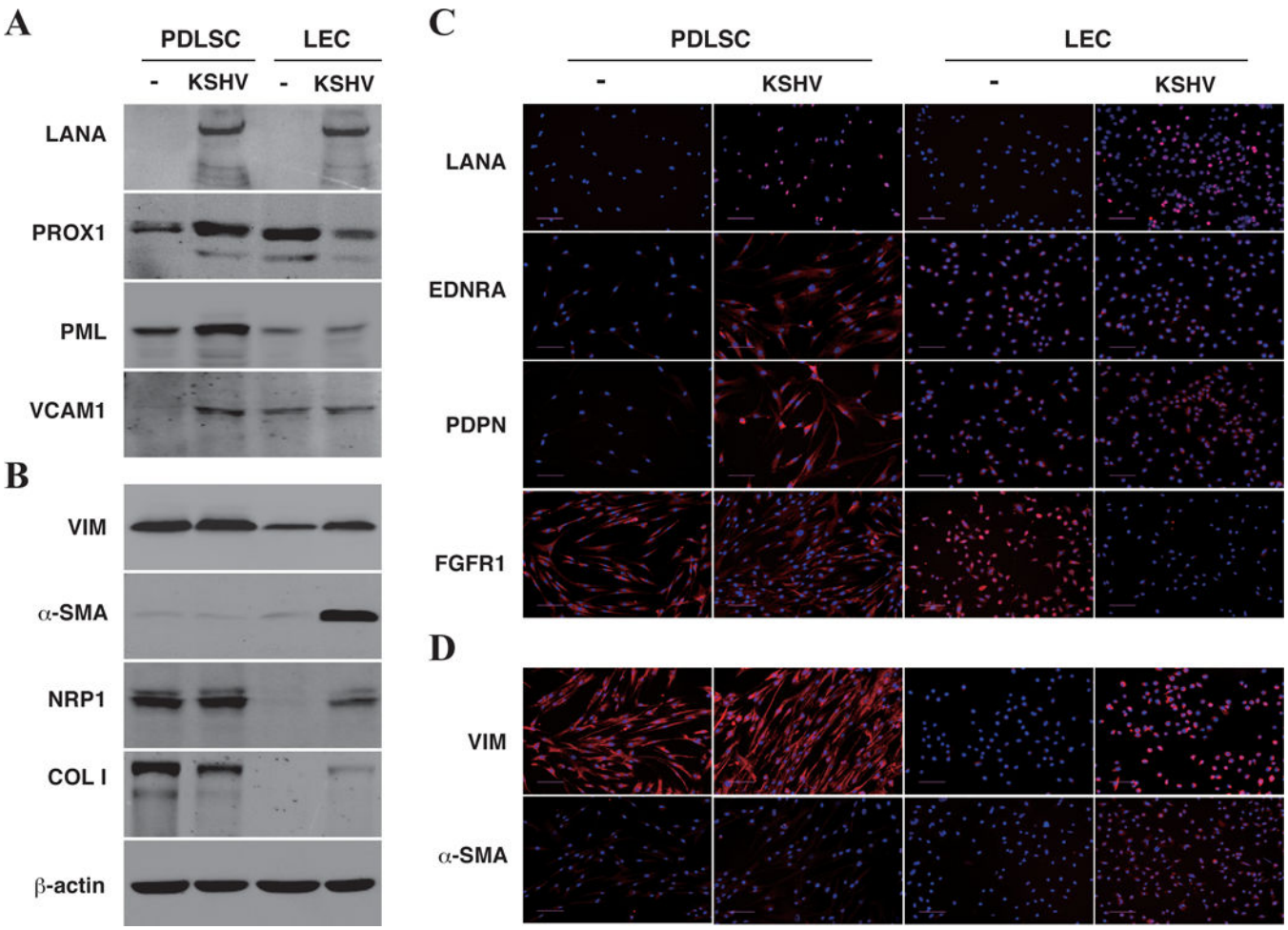

Fig. 7. Expression of MEndT and EndMT related gene in PDLSCs and LECs in response to KSHV infection

PDLSCs and LECs were infected with KSHV in an MOI of 50 (viral genomic DNA equivalent). Ninety-six hours post-infection, mock- and KSHV-infected cells were collected and analyzed by Western Blotting (A and B) or seeded in coverslips and subjected to IFA (C and D) with antibodies specified.